

Changes in extremes and hydroclimatic regimes in the CREMA ensemble projections

Filippo Giorgi · Erika Coppola · Francesca Raffaele ·
Gulilat Tefera Diro · Ramon Fuentes-Franco ·
Graziano Giuliani · Ashu Mangain ·
Marta Pereira Llopart · Laura Mariotti · Csaba Torma

Received: 26 April 2013 / Accepted: 15 March 2014 / Published online: 12 April 2014
© Springer Science+Business Media Dordrecht 2014

Abstract We analyze changes of four extreme hydroclimatic indices in the RCP8.5 projections of the Phase I CREMA experiment, which includes 21st century projections over 5 CORDEX domains (Africa, Central America, South America, South Asia, Mediterranean) with the ICTP regional model RegCM4 driven by three CMIP5 global models. The indices are: Heat Wave Day Index (HWD), Maximum Consecutive Dry Day index (CDD), fraction of precipitation above the 95th intensity percentile (R95) and Hydroclimatic Intensity index (HY-INT). Comparison with coarse (GPCP) and high (TRMM) resolution daily precipitation data for the present day conditions shows that the precipitation intensity distributions from the GCMs are close to the GPCP data, while the RegCM4 ones are closer to TRMM, illustrating the added value of the increased resolution of the regional model. All global and regional model simulations project predominant increases in HWD, CDD, R95 and HY-INT, implying a regime shift towards more intense, less frequent rain events and increasing risk of heat wave, drought and flood with global warming. However, the magnitudes of the changes are generally larger in the global than the regional models, likely because of the relatively low “climate sensitivity” of the RegCM4, especially when using the CLM land surface scheme. In addition,

This article is part of a Special Issue on “The Phase I CORDEX RegCM4 Experiment Matrix (CREMA)” edited by Filippo Giorgi, William Gutowski, and Ray W. Arritt.

Electronic supplementary material The online version of this article (doi:10.1007/s10584-014-1117-0) contains supplementary material, which is available to authorized users.

F. Giorgi (✉) · E. Coppola · F. Raffaele · G. T. Diro · G. Giuliani · L. Mariotti · C. Torma
Abdus Salam International Centre for Theoretical Physics, Trieste, Italy
e-mail: giorgi@ictp.it

R. Fuentes-Franco
Center for Scientific Research and Higher Education (CICESE), Ensenada, Baja California, Mexico

A. Mangain
Centre for Atmospheric Sciences, Indian Institute of Technology Delhi, New Delhi, India

M. P. Llopart
Department of Atmospheric Sciences, University of São Paulo, Rua do Matão, 1226, Cid. Universitária, São Paulo, SP 05508-090, Brazil

pronounced regional differences in the change signals are found. The data from these simulations are available for use in impact assessment studies.

1 Introduction

Knowledge of changes in hydroclimatic extreme statistics in response to climate change induced by anthropogenic greenhouse gases (GHG) is essential for the assessment of impacts and vulnerability to global warming (IPCC 2012). Analysis of extensive model results has shown that various types of extremes are expected to increase with global warming, such as drought, flood and heat waves (IPCC 2012; Sillmann et al. 2013). In fact, some studies suggest that global warming might induce fundamental changes in the characteristics of the Earth's hydrologic cycle and related hydroclimatic regimes (e.g. Trenberth 1999; Giorgi et al. 2011).

Simulation of hydroclimatic extremes optimally requires high model resolution, both spatial and temporal, hence high resolution regional modeling represents an important context for assessing the response of extreme events to global warming (Giorgi and Mearns 1999). Indeed, a number of papers have assessed extreme events in ensembles of Regional Climate Model (RCM) simulations for specific regions (e.g. Beniston et al. 2007; Kjellstrom et al. 2007; Lenderink 2010; Nikulin et al. 2012). Therefore, the CORDEX RegCM hyper-Matrix (CREMA) ensemble described in this special issue (Giorgi 2014, this issue) offers a good opportunity to explore changes in extreme events in long term regional climate projections across different domains and model configurations.

In this paper we analyze different hydroclimatic extreme indices based on temperature and precipitation daily data in the CREMA ensemble of transient projections, and attempt in particular to identify common behaviors across the different domains and simulations. The extremes are calculated for both the RCM and corresponding driving Global Climate Model (GCM) experiments in order to identify whether the higher resolution of the RCMs might lead to different or common conclusions compared to the coarser resolution GCMs. Both, the performance of the models in present day climate conditions and the changes in extreme indices are investigated. Here we present summary results for all CREMA experiments, while specific in-depth analysis of individual domains and events (e.g. tropical cyclones) is left to companion papers of this special issue. Also, we recall that an overall assessment of the models' biases and change signals is presented in the companion paper by Coppola et al. (2014, this issue).

2 Experiment and analysis design

2.1 The RegCM4 model

The CREMA ensemble was produced using the latest version of the Abdus Salam International Centre for Theoretical Physics (ICTP) regional climate model RegCM4 (Giorgi et al. 2012). This version represents the latest evolution of previous ones (Pal et al. 2007), with upgrades in most aspects of the model physics and a major rewriting and optimization of the code. The model is hydrostatic and includes a number of options for physics parameterizations (Giorgi et al. 2012), from which those used in the CREMA simulations were selected (Coppola et al. 2014, this issue). In particular, in the runs discussed here the model describes land surface processes using either the Biosphere- Atmosphere Transfer Scheme (BATS, Dickinson et al.

1993) or the Common Land Surface model (CLM3.5, Oleson et al. 2008), and convective precipitation using either the scheme of Grell (1993) or that of Emanuel and Rothman (1999).

2.2 The CREMA ensemble

Table S1 (Supplementary material) describes the CREMA ensemble. All simulations are performed with the RegCM4 using different physics schemes, and extend from 1970 to 2100. Simulations for two Representative Concentration Pathways (RCPs, Moss et al. 2010) were carried out, RCP4.5, a mid level pathway, and RCP8.5, a high level one. However, in this paper for brevity the analysis is presented only for the RCP8.5 scenario, bearing in mind that similar general conclusions were found for the RCP4.5 one (not shown).

Projections were completed for 5 CORDEX domains, Africa, South America, Central America, South Asia and Mediterranean (see Figure S1), and each domain follows the CORDEX specifications (Giorgi et al. 2009) which entail a horizontal grid spacing of 50 km. Note that, for each domain, at least two different model configurations are used (mostly either BATS-Grell or CLM-Emanuel, see Table S1), which were chosen based on a series of preliminary experiments (see Giorgi 2014, this issue). Driving GCMs include the Hadley Center HadGEM2-ES (HadGEM), the Max-Planck Institute for Meteorology MPI-ESM-2R (MPI) and the Geophysical Fluid Dynamics GFDL-ESM2M (GFDL), all taken from the CMIP5 ensemble (Taylor et al. 2012). They were chosen among those available at the time of the completion of these runs on the basis of their good performance in reproducing temperature and precipitation patterns over the selected domains (see also Giorgi 2014 this issue).

2.3 Extreme indices

We here analyze 4 indices of temperature and precipitation extremes, defined as:

Heat Wave Day Index (HWD): Number of heat wave days, where a heat wave occurs when for at least N_d consecutive days the daily maximum temperature exceeds the long term average by at least N_t degrees.

Dry Spell Length Index (CDD): Maximum number of consecutive dry days, where a dry day is defined as having precipitation below 1 mm/day.

Heavy precipitation Index (R95): Percent of total precipitation above the 95 % percentile.

Hydroclimatic Intensity Index (HY-INT): Product of normalized mean precipitation intensity and normalized mean dry spell length.

All indices are calculated using data for the entire year. The first three indices were selected from the standard set recommended by the World Meteorological Organization, and represent some of the key indices for impact assessment studies. The HY-INT index was introduced by Giorgi et al. (2011) and is a measure of change in hydroclimatic regimes, with increasing HY-INT implying a shift towards a regime of more intense and less frequent precipitation events.

The performance of the models in reproducing present day statistics of the precipitation indices is assessed against two observation datasets, the daily mean precipitation dataset at $0.25 \times 0.25^\circ$ horizontal resolution from the Tropical Rainfall Measuring Mission (TRMM VB42V46; Huffman et al. 2007; hereafter referred as TRMM and available for the period 1998–2009) and the One-Degree Daily (1DD) data of GPCP V1.1 (GPCP1; Huffman et al. 2001; hereafter referred as GPCP and available from 1996 to 2004). The reference period for the model assessment is 1976–2005. Note that the observations are available only for shorter

periods (almost overlapping with each other) than the simulation reference one. We nevertheless decided to use the longer simulation period in the analysis in order to have more robust statistics and because, without data assimilation, the model reference period does not refer to the actual observed one (i.e. the model 1996–2004 is not the real 1996–2004). Although it is possible that interdecadal variability might affect to some extent this evaluation, its effect is likely small for the first order analysis presented here. For temperature we do not have available gridded observed daily data that cover sufficiently well all of our domains, and therefore we limit our analysis to the change signal.

3 Results

3.1 Assessment of precipitation indices for the present day reference period 1976–2005

In this section we first present an assessment of the RegCM4 and corresponding GCM simulations of the two indices CDD and R95. Figures 1 and 2 compare these indices averaged over the period 1976–2005 for the RegCM4 and GCM simulations and over the periods of available data in the case of GPCP, and TRMM. All 5 CORDEX domains considered are shown, and in those regions where they overlap, the domain is selected which is specifically designed to best represent that region under the CORDEX protocol. For example, over the northern areas of South America covered by both the Central and South America domains, the latter is shown. For the models, ensemble average data for all simulations are presented.

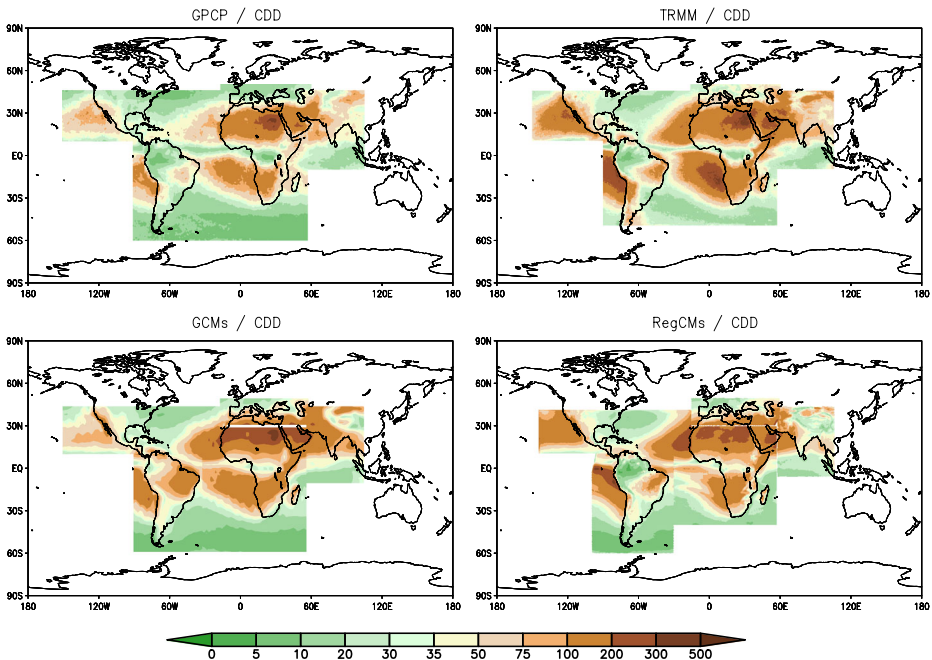


Fig. 1 Mean value of CDD over the five CREMA domains for GPCP (1996–2004; upper left panel), TRMM (1998–2009; upper right panel), GCM ensemble (1976–2005; lower left panel), RegCM4 ensemble (1976–2005, and RegCM lower left panel). Units are No. days

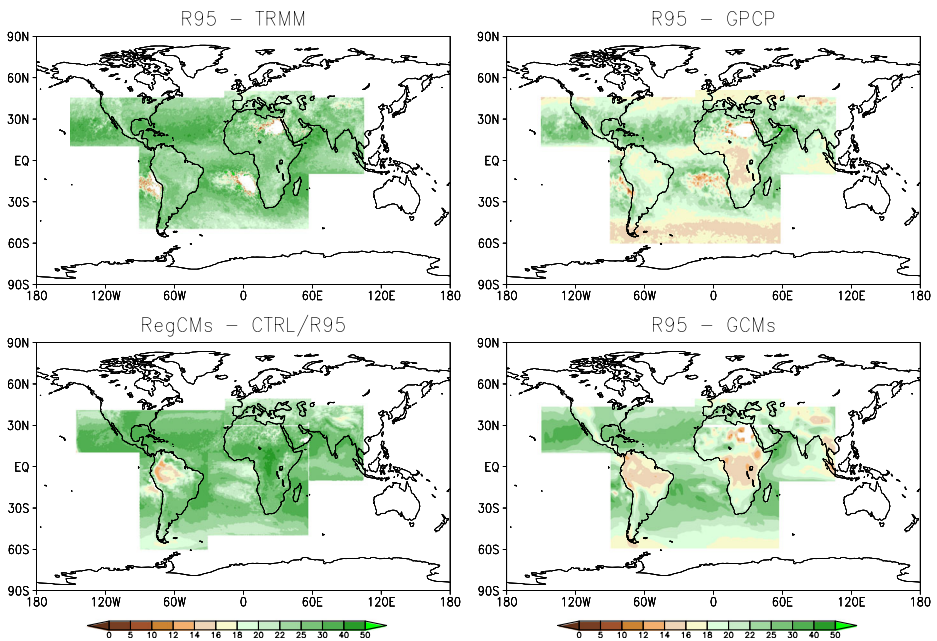


Fig. 2 Mean value of R95 over the five CREMA domains for GPCP (1996–2004; *upper right panel*), TRMM (1998–2009; *upper left panel*), GCM ensemble (1976–2005; *lower right panel*), RegCM4 ensemble (1976–2005, and *RegCM lower left panel*). Units are %

Concerning the CDD, we first find a generally good consistency between the GPCP and TRMM data. In the regions covered by the RegCM4 domains observed maxima of CDD are found over the Sahara and Southern Africa regions, the southwestern regions of North America, the southwestern coastal regions of South America and eastern Brazil, the middle east and central Asia. Conversely, observed minima occur over the southeastern regions of North America, the central/northwestern Amazon and La Plata Basin, equatorial Africa and, to a lesser extent, central/eastern India.

Comparison of the observed and simulated CDD patterns shows a generally good performance by the two ensembles. The GCM set reproduces rather well the broad global CDD pattern, and the regionalization by the RegCM4 captures some observed regional signals over the simulation domains. In fact, we highlight a few areas where the RegCM4 ensemble appears to improve the field from the GCMs: in South America the GCMs fail to reproduce the minimum over the western Amazon Basin, which is better captured by the RegCM4 ensemble; similarly, the La Plata basin maximum is better defined in the RegCM4; over the India continent the GCMs substantially overestimate the CDD, while the RegCM4 ensemble is closer to observations.

Figure 2 shows observed and simulated (ensemble averaged) R95, and offers some interesting considerations. First, differently from the CDD, we find substantial differences between the two observation datasets, with the TRMM data yielding generally larger values than GPCP. Notwithstanding possible differences in the calibration procedures of the two datasets, this is very likely a result of the higher resolution of the TRMM data. A comparison of the model ensembles with the observation data shows that the RegCM4 runs are closer to the TRMM data, while the GCMs are closer to the GPCP data. This is consistent with the

differences in resolutions across the two simulation ensembles and illustrates the added value of going to higher resolution using a nested RCM.

To better illustrate this point we selected four land regions (see Figure S1) and constructed Empirical Probability Density Functions (EPDFs) of daily precipitation for all individual runs and observation datasets, incorporating in the EPDFs all land grid points in these regions. The EPDFs are shown in Fig. 3. In all regions we see a separation between the fine and coarse scale EPDFs, both in the observation and simulation datasets. For example, in West Africa both the GPCP and GCM data produce events that at most reach about 100 mm/day, with the GCMs somewhat overestimating light events and underestimating the occurrence of the heaviest events compared to GPCP. The RegCM4 runs produce a much longer tail more in line with the TRMM data, although compared to this dataset the model overestimates the occurrence of the heaviest events and underestimates the frequency of events in the middle of the distribution. The model produces a small number (note the logarithmic scale) of events in excess of 350–400 mm/day, possibly because of the occasional occurrence of what have been defined “numerical point storms” (e.g. Giorgi 1991). However the RegCM4 shows a much closer EPDF to the high resolution observation dataset than the GCMs.

For the India and La Plata basin cases the RegCM4 runs can reproduce the tail of the observed TRMM distribution, while the GCMs show less intense extreme events more in line with the GPCP data. In fact, for these two regions, the TRMM and RegCM4 tails are in relatively good agreement while, similarly to the West Africa region, the model underestimates the frequency of events in the middle of the distribution. Finally, in the Central America region (Fig. 3d) not only do we find a separation between the coarse and fine scale EPDFs, but also a quite different behavior between two sets of RegCM4 runs, i.e. the BATS-Grell simulations closely reproduce the TRMM EPDF, while the CLM-EM ones overestimate the observed EPDF virtually across the entire distribution (in line with the overestimate of mean precipitation found in Coppola et al. 2014), the BATS Grell reproduces it quite well.

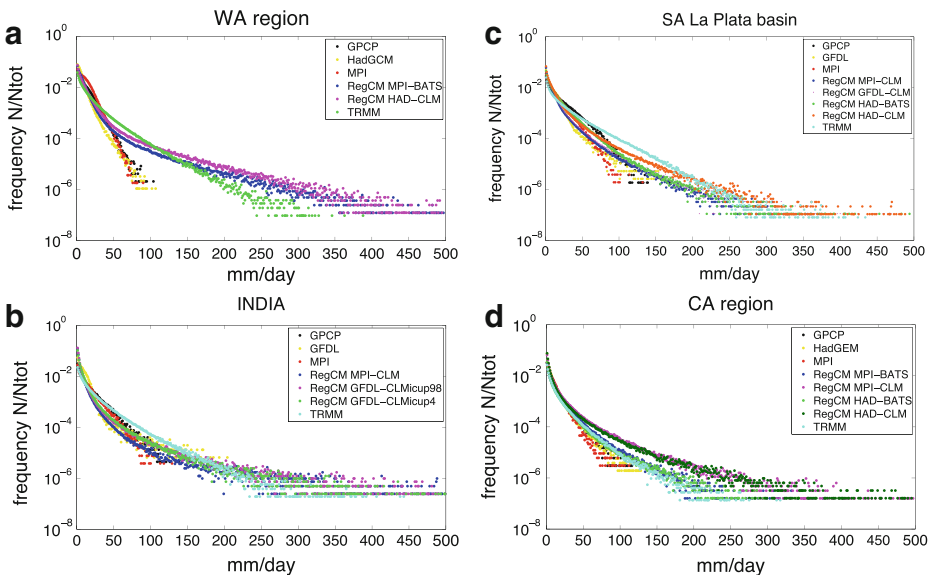


Fig. 3 Empirical distribution of daily precipitation events for TRMM, GPCP, and individual GCM and RegCM simulations for the four regions depicted in Figure S1. **a** West Africa; **b** Central India; **c** La Plata Basin; **d** upper Central America

We therefore find that the regional model produces values of CDD and R95 that are generally in line with the high resolution TRMM data and yields and improvement in the simulation of the precipitation EPDFs (compared to the driving GCMs) expected from its increased resolution. Conversely, the GCMs selected provide results that are generally in line with the coarser resolution GPCP dataset, although in this case the occurrence of most extreme events appears mostly underestimated.

3.2 Changes in extreme event indices

In this section we discuss changes (2071–2100 minus 1976–2005, RCP8.5 only) and/or 21st century trends (linear trends over the 2005–2100 period) in the 4 indices described in Section 2. We present both spatial maps of the ensemble average changes/trends (Figs. 4, 5, 6 and 7) and changes for individual simulations averaged over the continental areas within each domain (Tables S2–S4). In Figs. 4, 5, 6 and 7 the ensemble average for each domain is calculated using all available RegCM4 and corresponding driving GCM experiments for that domain.

Coppola et al. (2014, this issue) discuss the ensemble average changes in mean annual temperature and precipitation and these are reported in the supplementary Figure S2. Concerning temperature, in general the RegCM4 runs exhibit somewhat lower warming magnitudes than the GCM ensemble, i.e. the RegCM4 has a relatively low “climate sensitivity”, especially when using the CLM scheme (Coppola et al. 2014, this issue). For precipitation, the broad scale patterns of change in the two ensembles are similar (although with different regional detail) and can be summarized as follows: decreased precipitation over

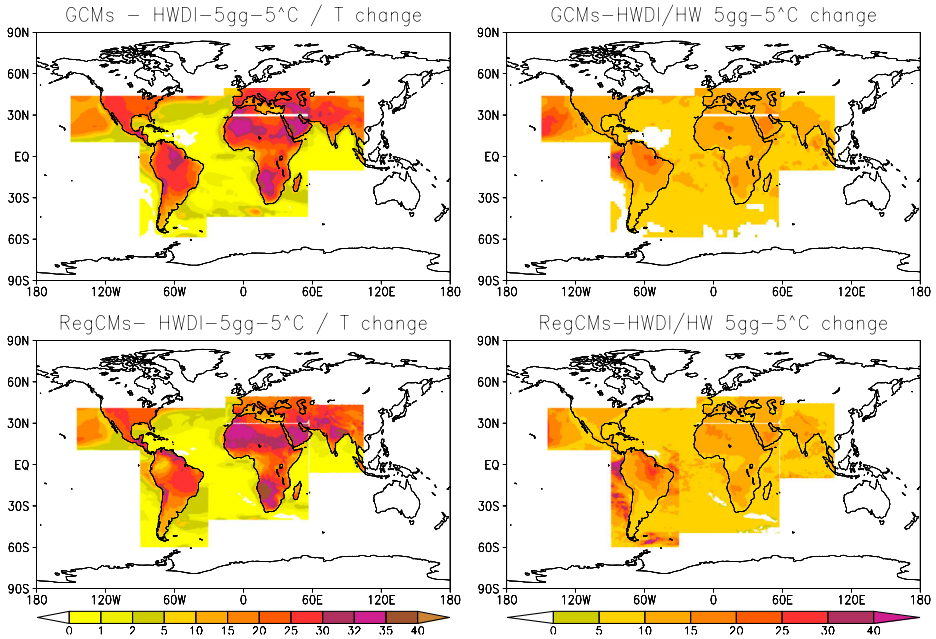


Fig. 4 Ensemble mean change (2071–2100 minus 1976–2005) in heat wave characteristics for the thresholds $N_d=5$ days and $N_t=5$ °C over the five CREMA domains. Upper panels show the GCM runs, lower panels show the RegCM4 runs. Left column: change in number of HWD (compared to present day means) per year per degree of (local) warming. Right column: change in mean heat wave length in days

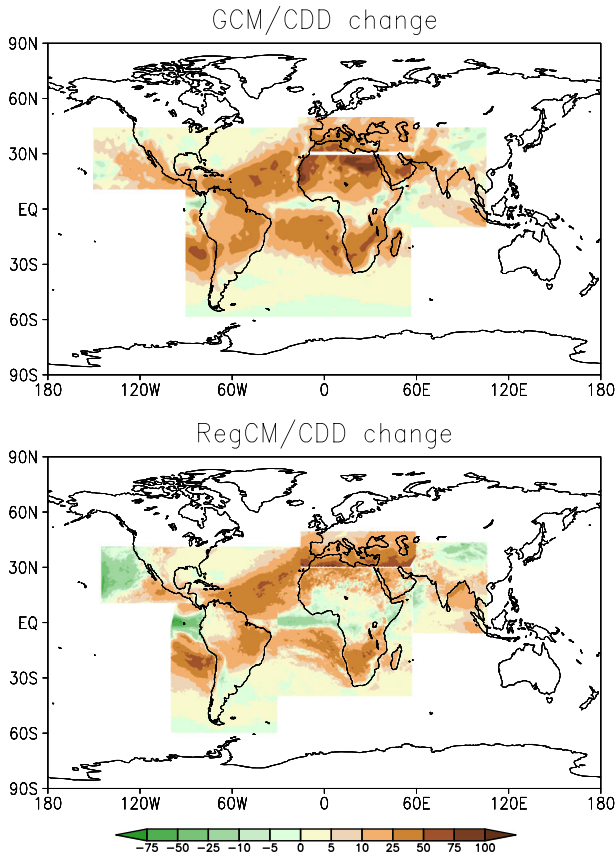


Fig. 5 Ensemble mean change (2071–2100 minus 1976–2005) in CDD over the five CREMA domains. The CDD is calculated for each year and then averaged over the 30-year period. Upper panel shows the GCM runs, lower panel shows the RegCM4 runs. Units are No. Days

central America, the northeastern and eastern regions of Brazil, the western coastal areas of West Africa, southern Africa, the Mediterranean and areas of central India (more extended in the RegCM4 than the GCMs); increased precipitation over the southeastern United States, la Plata basin, areas of equatorial and east Africa (more extended in the GCMs), Southern India. The reader is referred to Coppola et al. (2014, this issue) for more detail.

3.2.1 Heat wave day index (HWD)

As mentioned above, the heat wave index depends on two threshold parameters, the number of consecutive days N_d exceeding an anomaly of N_t degrees C. Figure 4 shows the ensemble average change in number of heat wave days (HWD) per year per degree of (local) warming, along with the mean length of heat wave, when both N_d and N_t are equal to 5, which is a standard value used for example by Tebaldi et al. (2006) and Meehl et al. (2007). The HWD is calculated using the daily maximum temperature (TMAX) with respect to the reference mean TMAX, and therefore is affected by mean warming as well as changes in variability. Also, for simplicity we use the same

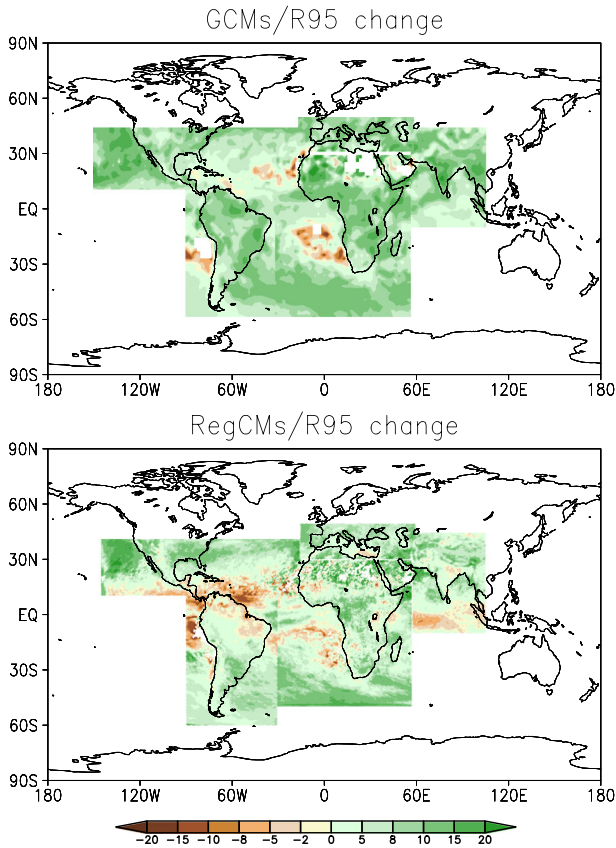


Fig. 6 Ensemble mean change (2071–2100 minus 1976–2005) in R95 over the five CREMA domains. The R95 is calculated for each year and then averaged over the 30-year periods. Upper panel shows the GCM runs, lower panel shows the RegCM4 runs. Units are %

HWD definition for all domains, however it was pointed out by one reviewer that different values of N_t and N_d might be more suitable over different regions. Results are shown for both the RegCM4 and corresponding GCM ensembles. Table S2 reports the corresponding changes in number of heat wave days averaged over five continents (land only) for each individual run.

The number of HWD increases over all regions due to the general warming projected by the models, with maximum increases of up to 25–30 days/year over the Amazon Basin, Sahara, Southern Africa, central India and Mediterranean. At the continental average scale (Table S2) the changes are in the range of 20–30 days/year. In general both Fig. 4 and Table S2 show that the change in number of heat wave days is somewhat larger in the GCMs than the RegCM4 simulations. This is mostly because, as mentioned above, the regional model produces lower warming than the GCMs (Figure S2). The most noticeable exception is the central India region, where the RegCM4 shows a greater change due to a greater projected decrease of precipitation there (Figure S2). Compared to BATS, CLM is characterized by a weaker response to atmospheric forcing and a lower climate sensitivity, which results in lower increases of HWD (Table S2).

A greater agreement between GCMs and RegCM4 is found in terms of changes in mean length of heat waves (Fig. 4, right column), which are mostly in the range of 5–15 days compared to values in the reference period mostly in the range of ~5–10 days. Most prominent

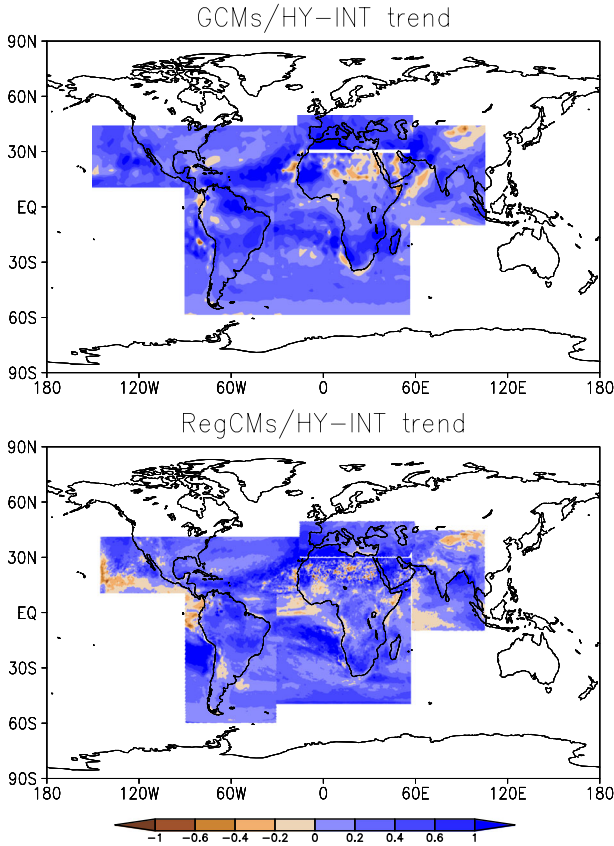


Fig. 7 Ensemble mean trend (2005–2100) in the index HY-INT over the five CREMA domains. The HY-INT is calculated for each year and then the trend is computed using these annual values (as in Giorgi et al. 2011). Upper panel shows the GCM runs, lower panel shows the RegCM4 runs. Units are % change

is the maximum change seen over the eastern Amazon and Brazil, a hot spot present in both ensembles. Figure S3 illustrates the sensitivity of the change in HWD to N_t and N_d , by showing changes for the three cases $N_t=5, N_d=10$; $N_t=10, N_d=5$; $N_t=10, N_d=10$, i.e. cases in which either one or both of the parameters are doubled. The last case would be indicative of the occurrence of extremely severe heat waves in which anomalies of at least $10\text{ }^\circ\text{C}$ would persist for at least 10 days. When only N_d is increased to 10 days, we do not find strong differences with respect to Fig. 4, while the increase in HWD is reduced when N_t is increased to 10 $^\circ\text{C}$ with change values mostly less than 5 HWD/year. This suggests that the main factor affecting the increase of HWD (with respect to present day climatology) is the mean warming, rather than the occurrence of peak temperature anomalies, a result which is in agreement with some previous studies (Ballester et al. 2010a, b). Note in Figure S3 the emergence of the Amazon Basin as a prominent hotspot in terms of heat wave enhancement.

3.2.2 Precipitation extreme indices

Figures 5 and 6 show the ensemble average changes (2071–2100 minus 1976–2005) for the CDD and R95 indices, while Tables S3–S4 present the continental average corresponding values. It is

evident that for all domains most areas exhibit positive values for both the CDD and R95 indices. Comparison of these figures with the mean annual precipitation change (Figure S2) shows that the areas of positive CDD (R95) change are greater than the areas of negative (positive) precipitation change. This implies that the increase in dry and wet extremes is not specifically tied to the precipitation change, but reflects a possible shift in hydroclimatic regime, which we will explore in greater detail in the next section.

Intercomparison between the GCM and corresponding RegCM4 runs (Figs. 5 and 6 and Tables S3–S4) shows that for both indices the GCM changes are of systematically larger magnitude than the RegCM4 ones, essentially in all domains. It is difficult to clearly identify the causes of this difference. One is likely that, as mentioned, the RegCM4 produces lower warming than the GCMs (Figure S2, Coppola et al. 2014, this issue).

Comparison of different RegCM4 configurations (Tables S3–S4) also shows some systematic behaviors, most noticeably the fact that the CLM-EM configuration tends to produce lower magnitude responses in CDD and R95 than the BATS-Grell one, particularly over tropical domains. We attribute this to the use of CLM vs. BATS, since previous experience by the authors has shown that the BATS scheme has a stronger response and feedback with the atmospheric forcing than CLM, likely because of the use of a force-restore soil model rather than a multi-layered one as in CLM. This enhanced feedback would especially contribute in amplifying wet and dry extremes (e.g. Seneviratne et al. 2006).

In terms of regional distribution, areas that show maximum increase in CDD include Eastern Brazil, Southern Africa, Central America, the Mediterranean and the Indian continent, while a decrease in CDD is found over the La Plata basin, western Amazon, Congo Basin and Eastern and western United States, clearly in response to an increase of simulated precipitation there (Figure S2). Concerning the R95 change, areas of maximum increase largely correspond to areas of increased precipitation, while some areas of decrease are found in the RegCM runs (e.g. eastern Brazil) in correspondence with a strong precipitation reduction.

3.2.3 HY-INT index

Giorgi et al. (2011) introduced the HY-INT index as a measure of the global warming-induced shift of the hydrologic cycle towards a regime of more intense and less frequent precipitation events. They found positive trends of HY-INT in a range of 21st century global and regional model projections. Figure 7 shows the 21st century trends in HY-INT calculated for the GCM and RegCM4 CREMA RCP8.5 projections. This trend is positive almost everywhere, both for the GCMs and RegCM4 experiments, with linear trend values for the period 2005–2100 in line with those found by Giorgi et al. (2011). Consistently with what found for the other indices, we find generally larger HY-INT trends in the GCM than the RegCM4 simulations, mostly because of the relatively low values found in the CLM runs.

Therefore, the present GCM and CORDEX simulations confirm the conclusion of Giorgi et al. (2011) of the increase in HY-INT being a strong and ubiquitous indicator of the response of the earth's hydrologic cycle to global warming.

4 Conclusions

In this paper we analyze present day and future changes in four hydroclimatic extreme and regime indices in the GCM and RegCM4 ensembles of the Phase I CREMA experiment for the RCP8.5 GHG concentration scenario (Giorgi 2014 this issue). Comparison of the present day simulation period with two precipitation observation datasets (the high resolution TRMM

and coarse resolution GPCP) shows that, while the GCM daily precipitation distributions are in line with the coarse resolution GPCP observations, the RegCM4 ones are more consistent with the TRMM dataset, particularly in exhibiting a much longer tail of the distribution (high precipitation events) and a better representation of dry day sequences. This result illustrates the added value of the higher resolution of the regional model. In fact, the aim of a downscaling exercise is to provide realistic fine scale information which enhances that of the coarse scale GCMs, and in our case, this added information (in spectral space) is represented by the tails of the daily precipitation distribution. Our experiment is thus well illustrative of the aim of downscaling: the GCMs reproduce the coarse scale EPDFs (GPCP) while the regional model better reproduces the fine scale EPDFs (TRMM). Concerning the change signal, both the GCMs and RCMs show a prevailing increase of CDD and R95, regardless of the change in mean precipitation. Therefore both sets of models suggest greater occurrence of drought-prone and flood-prone conditions. In addition a pronounced increase in heat waves (compared to present day climatology), both duration and intensity, is simulated, largely tied to the mean warming. Finally, a predominant positive trend in HY-INT is found in the ensemble indicating a regime shift towards more intense and less frequent precipitation events.

Recently, Donat et al. (2013) analysed observed 20th century trends in a series of temperature and precipitation indices, including R95 and CDD. It is very difficult to compare our results with those of Donat et al. (2013), since they included trends only for some sub-regions of our domains where data were available and show trends with marked spatial variability. However our results are in line with their finding of a prevalence of areas with increasing precipitation intensity. On the other hand, our spatial patterns of change in R95 and CDD are generally in line with those of Sillmann et al. (2013) for the full CMIP5 set of experiments, a further indication that our sub-set of GCMs is representative of the CMIP5 ensemble. Finally, in this paper we discussed only ensemble averaged results, but a relatively large inter-model spread of results was found, both across GCMs and across RegCM4 physics configurations. Other papers in this special issue analyze in detail inter-model differences of response over the different domains.

Comparison of GCM vs. RegCM4 results showed that the changes produced by the GCMs were generally of larger magnitude than those produced by the RegCM4. This is at least partially because of the relatively lower surface warming exhibited by the regional model, especially when using the CLM land surface scheme. In order to increase the robustness of our projections, we plan to continue to populate the CREMA ensemble with further CORDEX simulations and to make available the results from these simulations for eventual use in impact assessment studies.

Acknowledgments This work was partially supported by grants from the project NextDATA funded by the Italian Consiglio Nazionale della Ricerca (CNR).

References

- Ballester J, Giorgi F, Rodo X (2010a) Changes in European temperature extremes can be predicted from changes in PDF central statistics. *Clim Chang Lett* 98:277–284
- Ballester J, Rodo X, Giorgi F (2010b) Future changes in central Europe heat waves to mostly follow summer mean warming. *Clim Dyn* 35:1191–1205
- Beniston M et al (2007) Future extreme events in European climate: an exploration of regional climate model projections. *Clim Chang* 81:71–95
- Coppola E et al. (2014) Present and future climatologies in the Phase I CREMA experiment. *Climatic change*, this issue

- Dickinson RE, Henderson-Sellers A, Kennedy PJ (1993) Biosphere—atmosphere transfer scheme, BATS: version 1E as coupled to the NCAR Community Climate Model. Technical Note NCAR/TN—387 + STR, 72p
- Donat MG et al (2013) Updated analyses of temperature and precipitation extreme indices since the beginning of the twentieth century: the HadEX2 dataset. *J Geophys Res—Atmos* 118:20998–22118
- Emanuel KA, Rothman MZ (1999) Development and evaluation of a convection scheme for use in climate models. *J Atmos Sci* 56:1756–1782
- Giorgi F (1991) Sensitivity of summertime precipitation over the western United States to model physics parameterizations. *Mon Weather Rev* 119:2870–2888
- Giorgi F (2014) The Phase I CORDEX RegCM hyper-Matrix (CREMA) experiment. Introduction to the special issue. *Climatic Change*, this issue
- Giorgi F, Mearns LO (1999) Introduction to special section: regional climate modeling revisited. *J Geophys Res* 104:6335–6352
- Giorgi F, Jones C, Asrar G (2009) Addressing climate information needs at the regional level: the CORDEX framework. *WMO Bull* 175–183
- Giorgi F et al (2011) Higher hydroclimatic intensity with global warming. *J Clim* 24:5309–5324
- Giorgi F et al (2012) RegCM4: model description and preliminary tests over multiple CORDEX domains. *Clim Res* 52:7–29
- Grell GA (1993) Prognostic evaluation of assumptions used by cumulus parameterizations. *Mon Weather Rev* 121:764–787
- Huffman GJ et al (2001) Global precipitation at one-degree daily resolution from multi-satellite observations. *J Hydrometeorol* 2:36–50
- Huffman GJ et al (2007) The TRMM multisatellite precipitation analysis (TMPA): Quasi-global, multiyear, combined-sensor precipitation estimates at fine scale. *J Hydrometeorol* 8:38–55
- IPCC (2012) In: Field CB, Barros V, Stocker TF, Qin D, Dokken DJ, Ebi KL, Mastrandrea MD, Mach KJ, Plattner G-K, Allen SK, Tignor M, Midgley PM (eds) *Managing the risks of extreme events and disasters to advance climate change adaptation. A special report of Working Groups I and II of the Intergovernmental Panel on Climate Change*. Cambridge University Press, Cambridge, p 582
- Kjellstrom E et al (2007) Modeling daily temperature extremes: recent climate and future changes over Europe. *Clim Chang* 81:249–265
- Lenderink G (2010) Exploring metrics of extreme daily precipitation in a large ensemble of regional climate model simulations. *Clim Res* 44:151–166
- Meehl GA et al (2007) In: Solomon S (ed) *Global climate projections, chapter 10 of climate change 2007, The physical science basis, WGI contribution to the fourth assessment report of the intergovernmental panel on climate change (IPCC)*. Cambridge University Press, New York, pp 747–845
- Moss RH et al (2010) The next generation of scenarios for climate change research and assessment. *Nature* 463:747–756
- Nikulin G et al (2012) Precipitation climatology in an ensemble of CORDEX Africa regional climate simulations. *J Clim* 25:6057–6078
- Oleson K et al (2008) Improvements to the community land model and their impact on the hydrological cycle. *J Geophys Res* 113, G01021. doi:10.1029/2007JG000563
- Pal JS et al (2007) The ICTP RegCM3 and RegCNET: regional climate modeling for the developing world. *Bull Am Meteorol Soc* 88:1395–1409
- Seneviratne SI et al (2006) Land-atmosphere coupling and climate change in Europe. *Nature* 443:205–209
- Sillmann J, Kharin VV, Zwiers FW, Zhang X, Bronaugh D (2013) Climate extreme indices in the CMIP5 multimodel ensemble: Part 2. Future climate projections. *J Geophys Res—Atmos* 118:2473–2493
- Taylor KE, Stouffer RJ, Meehl GA (2012) An overview of CMIP5 and the experiment design. *Bull Am Meteorol Soc* 78:485–498
- Tebaldi C, Hayhoe K, Arblaster JM, Meehl GA (2006) Going to the extremes: an intercomparison of model-simulated historical and future changes in extreme events. *Clim Chang* 79:185–211
- Trenberth KE (1999) Conceptual framework for changes of extremes of the hydrological cycle with climate change. *Clim Chang* 42:327–339